

**Photometric, Spectroscopic and Orbital Period Study of
Three Early Type Semi-detached Systems:
XZ Aql, UX Her and AT Peg**

S. Zola^{1,2}

Astronomical Observatory, Jagiellonian University

Ö. Baştürk³

Ankara University, Faculty of Science

A. Liakos⁴

National Observatory of Athens

K. Gazeas⁵

National & Kapodistrian University of Athens

H. V. Şenavcı³

Ankara University, Faculty of Science

R. H. Nelson^{6,7}

Guest investigator, Dominion Astrophysical Observatory

İ. Özavcı³

Ankara University, Faculty of Science

B. Zakrzewski²

Mt Suhora Observatory, Pedagogical University

and

M. Yılmaz³

Ankara University, Faculty of Science

Received _____; accepted _____

¹Astronomical Observatory, Jagiellonian University, ul. Orla 171, PL-30-244 Krakow, Poland

²Mt Suhora Observatory, Pedagogical University, ul. Podchorazych 2, PL-30-084 Krakow, Poland

³Ankara University, Faculty of Science, Dept. of Astronomy and Space Sciences, Tandoğan, TR-06100, Ankara, Turkey

⁴Institute for Astronomy, Astrophysics, Space Applications and Remote Sensing, National Observatory of Athens, Penteli, Athens, Greece

⁵Department of Astrophysics, Astronomy and Mechanics, National & Kapodistrian University of Athens, Zografos, Athens, Greece

⁶1393 Garvin Street, Prince George, BC V2M 3Z1, Canada

⁷Dominion Astrophysical Observatory, Herzberg Institute of Astrophysics, National Research Council of Canada

ABSTRACT

In this paper we present a combined photometric, spectroscopic and orbital period study of three early-type eclipsing binary systems: XZ Aql, UX Her, and AT Peg. As a result, we have derived the absolute parameters of their components and, on that basis, we discuss their evolutionary states. Furthermore, we compare their parameters with those of other binary systems and with the theoretical models. An analysis of all available up-to-date times of minima indicated that all three systems studied here show cyclic orbital changes; their origin is discussed in detail. Finally, we performed a frequency analysis for possible pulsational behavior and as a result we suggest that XZ Aql hosts a δ Scuti component.

Subject headings: binaries: eclipsing - Stars: individual(XZ Aql, UX Her, AT Peg)

1. Introduction

Classification of eclipsing binaries is performed according to the physical and evolutionary characteristics of their components, in addition to the shapes of their light curves. The degree to which their inner critical equipotential surfaces (Roche lobes) have been filled is a critical parameter for their classification, which helps in the understanding of their physical nature. Semi-detached binaries constitute an important class of objects, with one component filling its Roche lobe. The shape of a typical semi-detached binary light curve is an Algol-type light variation. These objects are important in understanding this stage of evolution when the mass transfer starts to take place and alters the evolution of the components as single stars. Whether or not one or both of the components are in contact with their Roche lobes or very close to filling them is very important in understanding the evolution of interacting binary systems. In order to achieve this goal, light and radial velocity observations are analyzed to determine their absolute parameters (temperatures, masses, radii, and surface potentials in particular). If the mass transfer has started in these systems at some point during their evolution, it also manifests itself as orbital period changes because a transfer of mass would alter a system's moment of inertia.

In this study, we present the results of light curve and period change analyses of three Algol-type binary systems: XZ Aql, UX Her, and AT Peg. We derive their absolute parameters from the analysis of their light and radial velocity curves that we obtained at two different observatories. We analyze the differences between the observed (O) and the calculated (C) eclipse timings, occurring due to the changes in their orbital period, by constructing O-C diagrams. We also perform a frequency analysis to investigate the potential pulsation signals in the data of the studied systems. Finally, we discuss the evolutionary states of the components of these systems on Hertzsprung-Russell, Mass-

Luminosity and Mass-Radius diagrams (hereafter HRD, MLD, and MRD, respectively). Such thorough analyses for these systems were being performed for the first time within this study.

2. Systems

2.1. XZ Aql

XZ Aql (HD 193740, BD-07° 5271, GSC 5174-108, SAO 144345) is an Algol type eclipsing binary. It was discovered by Cannon (1922). The first detailed description of the light curve (without a plot) was presented by Witkowski (1925). Erleksova (1959) was the first (and, so far the only one) to present the graphical light curve and give the first discussion of the O-C diagram. She proposed two alternative models of the period variation: first, as an abrupt change between JD 2430000 and 2433000, and second as an increase at a constant rate. Pokorný & Zlatuška (1976) discussed the same subject, using a larger number of eclipse timings. Wood & Forbes (1963) and Samolyk (1996) noted a quadratic term in the ephemeris. A detailed discussion of shape of O-C diagram was given by Soydugan et al. (2006). They modeled the variation with a sinusoidal superimposed on a secular parabolic change. They attributed the sinusoid variation to the light time effect caused by an unseen third body, and the secular term to a conservative mass transfer from the less massive component to the more massive one, which had already been noted by previous studies. The orbital period of the hypothetical third body was $P_3 = 36.7 \pm 0.6$ yr. The spectral type of XZ Aql is A2, found by Cannon (1922) when the star was discovered. The mass ratio based on radial velocity observations has not been published until now, nor has any light curve solution.

2.2. UX Her

UX Her (HD 163175, BD+16° 3311, HIP 87643, SAO 103195, GSC 01557-01268) system was discovered by Cannon (Pickering 1908), who found its spectral type as B9 or A. Zinner (1913) confirmed the discovery and determined the correct period of the system. Later, Tsesevich (1944), Kaho (1952), Kurzemnietse (1952), Ashbrook (1952), Tsesevich (1954), Koch & Koch (1962), revised the elements. Gordon & Kron (1963) and Gordon & Kron (1965) published the first light curve solution based on the spectroscopic orbit determined by Sanford (1937) and their own photometric observations. They proposed that the secondary was an evolved, low-mass, late-type star. Hill et al. (1975) estimated the primary component’s spectral type as A0V - A3V for different orbital phases. Following the light curve studies of Cester et al. (1979), Mardirossian et al. (1980) and Giuricin & Mardirossian (1981), Lazaro et al. (1997) analyzed the first infrared light curves of the system in J, H and K bands, together with published B and V band light curves of Gordon & Kron (1965). They determined the parameters of the system and found that none of the components of the binary filled their Roche lobes. Although UX Her is a short-period system, they assigned it to a category of slightly detached systems, most of which, as they pointed out, were long-period systems. Djurašević et al. (2006) computed the mass ratio ($q = m_2 / m_1 = 0.248$) as the result of the q-search method. When combined with the results of their B and V band light curve analysis, this mass ratio value suggests a semi-detached configuration of UX Her.

Kurzemnietse (1952) noted for the first time that the period was variable. Tremko et al. (2004) first published a period-variation study of the system, which excluded a mass transfer between the components as the cause of the observed variations in the orbital period of the system, since neither of the stars filled their Roche lobes according to their

interpretation. They proposed that a low mass ($0.3 M_{\odot}$) unseen companion, bound to the system, was causing the period to change periodically.

2.3. AT Peg

Cannon (Cannon & Pickering 1924) published the first spectroscopic observation of AT Peg (HD 210892, BD+07° 4824, SAO 127380, GSC 1137-185), and determined its spectral type as A0. The variability of the system was first announced by Schneller (1931), who identified it as an Algol-type binary. Guthnick & Prager (1931), Rügemer (1934), Lassovszky (1935), Cristaldi & Walter (1963), Wood & Forbes (1963), Obürka (1964a), Obürka (1964b), Obürka (1965) and Cristaldi & Walter (1965) published their photometric observations and revised the light elements. Hill & Barnes (1972) published the orbital elements of the system based on the first detailed spectroscopic observations and determined the spectral type as A7 V. They found the mass ratio (m_1 / m_2) to be 2.4 and the orbital inclination $76^{\circ}.7$. Gülmen et al. (1993) found that AT Peg was a semi-detached binary with a later type subgiant secondary component filling its Roche lobe. Maxted et al. (1994) obtained spectra of the system and determined a spectroscopic mass ratio of 2.115 (m_1 / m_2), smaller than the one determined by Hill & Barnes (1972) from photographic plates. They determined absolute parameters of the system using the photometric observations of Cristaldi & Walter (1963). They also classified the spectral type of the primary component (A4 V) from a combined spectrum of their data, which was consistent with the temperature estimates obtained from Strömgren photometry by Hilditch & Hill (1975). The configuration of the system as a semi-detached eclipsing binary has been widely accepted since this study and that of Giuricin et al. (1981).

Savedoff (1951) was the first to notice that the orbital period was variable. Although the secular change in the eclipse timing variations has been noted by recent studies (Margrave 1981; Gudur et al. 1987; Liakos et al. 2012a; Hanna 2012), Liakos et al. (2012a) noticed also the discrepancy between the configuration and the direction of the mass transfer. They suggested either mass loss via stellar winds or system angular momentum loss via magnetic braking as possible explanations. Periodic variations in the O-C diagram have been also noted and attributed to unseen third bodies with parameters differing from one study to another (Borkovits & Hegedus 1995, 1996; Liakos et al. 2012a), or to magnetic activity with single (Sarna et al. 1997), or to multiple cycles (Hanna 2012). However there is no firm evidence for strong magnetic activity other than enhanced X-ray emission (Hanna 2012).

3. Observations

Between 2012 and 2013 we performed photometric observations of XZ Aql, UX Her, and AT Peg, using the 40-cm Cassegrain telescope (f/5 using a focal reducer) of the Gerostathopoulion Observatory of the University of Athens (UoA Observatory). This setup results in a field-of-view (FOV) of 17×26 arcmin. The telescope was equipped with with an SBIG ST-10 XME CCD detector and a set of *BVRI* filters (Bessell specifications) in order to perform multi-band photometry. We present a log of our observations in Table 1.

The ephemerides of all systems (see Table 2) were calculated using the least squares method on the minima timings derived from our observations and the most recent ones taken from the literature. The photometric data sets were reduced with dark and flat frames which were gathered before or after each observing run, while image reduction as well as differential aperture photometry were performed using either C-munipack (Hroch 1998; Motl 2004) or AIP4WIN (Berry & Burnell 2000) software packages. Comparison and check

stars are also listed in Table 2 together with their properties.

We acquired radial velocity measurements of our targets at the Dominion Astrophysical Observatory (DAO) in Victoria, British Columbia, Canada using the Cassegrain spectrograph attached on the 1.85 m Plaskett telescope. A grating (#21181) with 1800 lines/mm, blazed at 5000 Å giving a reciprocal linear dispersion of 10 Å/mm in the first order and covering a wavelength region from 5000 to 5260 Å approximately was used. A log of all spectroscopic observations is presented in Table 3. We used 'RaVeRe' software (Nelson 2010a) for cosmic hit removal, median background fitting and subtraction for each column, aperture summation, continuum normalization, wavelength calibration and linearization using the Fe-Ar spectra as wavelength standards. Finally, the radial velocities were extracted from the spectra by using the Rucinski broadening functions (Rucinski 2004; Nelson 2010b; Nelson et al. 2014) as implemented in the software 'Broad' (Nelson et al. 2014). In this process, IAU standard radial velocity stars, of spectral types F and G, were used to solve directly for the functions that account for the broadening and Doppler shifts of the spectra. In practice, a number of standard stars were used individually, and the mean values of the resulting radial velocities were adopted. In order to investigate the effect of the differing spectral types of the standard stars on the resulting radial velocities, we split

Table 1: Log of photometric observations

System	Dates of observations	Number of data points				Mean errors			
		B	V	R	I	$\sigma_B(\text{mag})$	$\sigma_V(\text{mag})$	$\sigma_R(\text{mag})$	$\sigma_I(\text{mag})$
XZ Aql	26 nights in Jun-Aug 2013	2282	2351	2405	2379	0.0091	0.0090	0.0086	0.0075
UX Her	10 nights in Jun 2012	2056	1986	1984	2028	0.0035	0.0032	0.0031	0.0034
AT Peg	6 nights in Aug 2012	895	895	895	895	0.0047	0.0054	0.0050	0.0054

the standard stars into two groups: one with F-types, and the other, G-types. Looking at the mean radial velocities derived from each group, we noted negligible differences between corresponding values—certainly less than the estimated errors. Therefore we did not deem it necessary to use different standard stars for primary and secondary spectra or to restrict the standard star choices in any other way.

AT Peg has previous radial velocity measurements using the 1.2 metre telescope at the DAO were reported in Maxted et al. (1994). Their determinations used an older technique involving a reticon detector and cross-correlations. We made use of their measurements in our analysis but did not combine both radial velocity data sets together because the V_γ values differ from one data set to another.

4. Analysis

4.1. Light Curve Modeling

In order to obtain initial parameters of the systems studied in this paper we used the Wilson-Devinney program augmented with the Monte Carlo search algorithm to ensure that the global minimum was found within the set ranges of free parameters. We followed the procedure outlined in Zola et al. (2014), that is keeping the values constant for systems’ mass ratios, as derived from sine fitting to the radial velocities. In the search for solutions,

Table 2: Ephemerides, magnitudes of the system, and the comparison and check stars

System	Epoch (T_0)	Period	m_v	(B-V)	Comparison			Check		
	(HJD+2400000)	(days)	(mag)	(mag)	GSC ID	m_v	(B-V)	GSC ID	m_v	(B-V)
XZ Aql	52501.0881	2.139207	10.18	0.25	5175-0726	10.48	0.96	5174-0186	10.87	0.73
UX Her	52501.5262	1.548869	8.97	0.15	1557-1029	9.21	0.89	1557-1196	9.73	0.99
AT Peg	52500.9285	1.146065	9.02	0.19	1137-0492	9.78	0.77	1137-0134	10.58	0.53

we adjusted inclination (i), temperature of the secondary (T_2), potentials ($\Omega_{1,2}$), luminosity of the primary star (L_1). Neither a spot nor a third light was required for the three targets analyzed in this work. In addition to the mass ratios, we also kept the temperatures of the primary components (T_1) constant following from the spectral type of a system. In order to determine T_1 , we used the spectral type versus temperature calibration published by Harmanec (1988). Furthermore, the albedo and gravity darkening coefficients were set at their theoretical values for either a radiative or a convective envelope. The limb darkening coefficients were built into the code and were chosen as a function of a star temperature and the wavelength of the observations from the tables by Claret & Bloemen (2011), Claret et al. (2012) and Claret et al. (2013) based on square root law. Due to the large number of observed single points, we calculated about 150 mean points for every binary and in each filter. These were calculated in such a way that they evenly covered the observed light curve and using ephemerides listed in Table 2. This procedure speeded up computations and also provided error estimates for each mean point. The convergence was achieved for all three systems and the resulted configurations (not assumed a priori) were all semi-detached with the secondaries filling the Roche lobe. In the next step we used the resulting parameters as starting ones in the simultaneous solution of light and radial velocity curves using the latest version, 2015 release (WD2015), of the Wilson-Devinney code (Wilson & Devinney 1971; Wilson 1979, 1990; Van Hamme & Wilson 2007; Wilson 2008; Wilson et al. 2010; Wilson 2012). We made use of the Mode-5 for the configuration, the usual mode for Algol-type binaries with the secondary component filling its Roche lobe in parallel with our findings for the configurations in the previous step. The list of free parameters was similar to those of the Monte Carlo search, however, also the mass ratio was adjusted as well as further two parameters describing the orbit: the semi-major axis of binary system relative orbit and the systemic velocity. We assumed that the orbits are circular due to strong tidal forces in case of semidetached systems. These computations were done with all individual points

and, setting the control parameter $KSD=1$, we made use of the program feature to let the program to compute the curve weights. Several iterations were required to derive the final, combined RV and LC solutions.

For AT Peg, we determined two separate solutions, one using RV data from Maxted et al. (1994), and the other, our own RV results. All the radial velocity observations and their fits obtained with the WD2015 code are given in Figs. 1 - 2. The results of the light curve analyses, as derived in the second step, are listed in Table 4 together with the formal error for each parameter in parenthesis as computed by the Wilson-Devinney code. The fits and their residuals are shown in Figs. 3 - 6. Finally, the computed absolute parameters are given in Table 5.

4.2. Orbital Period Analysis

In order to better understand the nature of studied systems, we constructed the O-C diagrams (Figs. 7 - 8) by using all minima times available in the literature together with those derived from our own observations, and weighting them according to the observation method (photographic: 0.3, visual: 0.5, photoelectric: 0.8, CCD: 1). We made use of the Kwee-van Woerden method (Kwee & van Woerden 1956) to derive the times of minimum light levels in our own light curves (Table 6).

Two out of the three systems: XZ Aql and AT Peg, show secular period changes, either period increase or decrease. The former may be an indication of mass transfer from the less massive to the more massive component or mass loss from the system while the latter, mass transfer in the opposite direction. We fitted the trends in period changes with parabolae, under the assumption of conservative mass transfer between components. Furthermore, we analyzed the residuals from the parabolic fit for two systems: XZ Aql and AT Peg. Cyclic

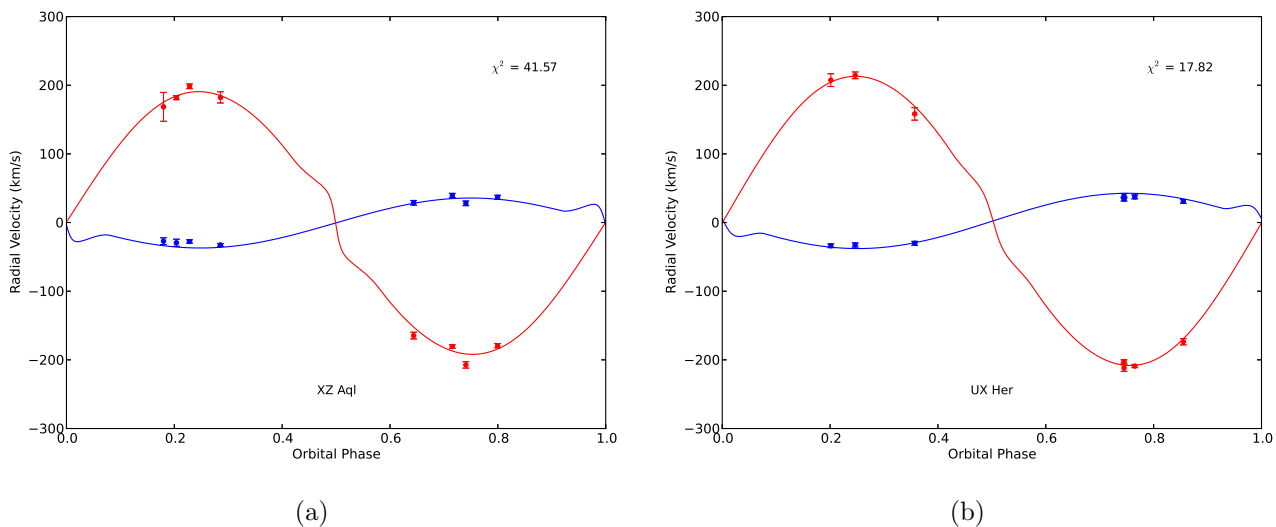


Fig. 1.— Observed radial velocity curves of XZ Aql (a) and UX Her (b). The best fits to compute radial velocity amplitudes K_1, K_2 are also given in solid lines. Systemic velocities have been subtracted from all the data.

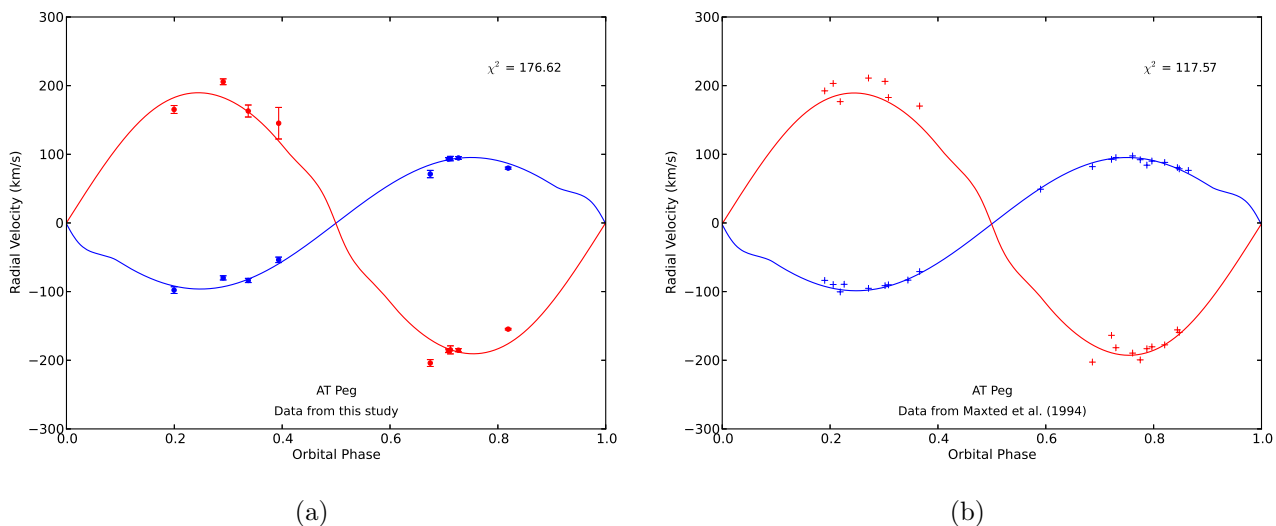


Fig. 2.— Same as in Fig. 1, but for two different data sets of AT Peg, our own measurements (a) and Maxted et al. (1994)’s measurements (b).

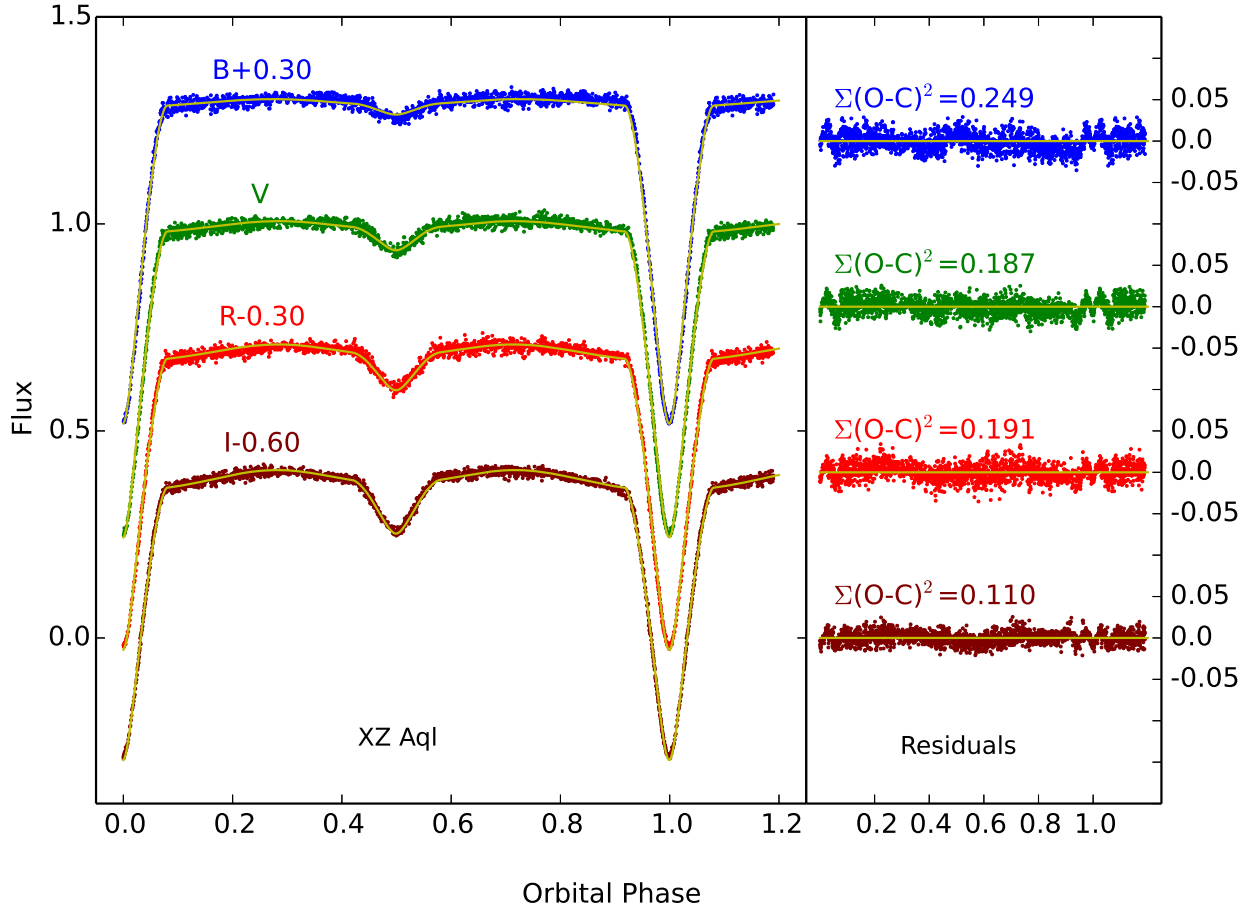


Fig. 3.— Observed light curves of XZ Aql. Data in *BVRI* filters (from top to bottom) were shifted arbitrarily by the amounts shown in figures for clarity. Theoretical light curves corresponding to the best fits are plotted in solid lines. Residuals from the fits are given at the right of the light curves using the same symbols, and shifted also arbitrarily as the light curves.

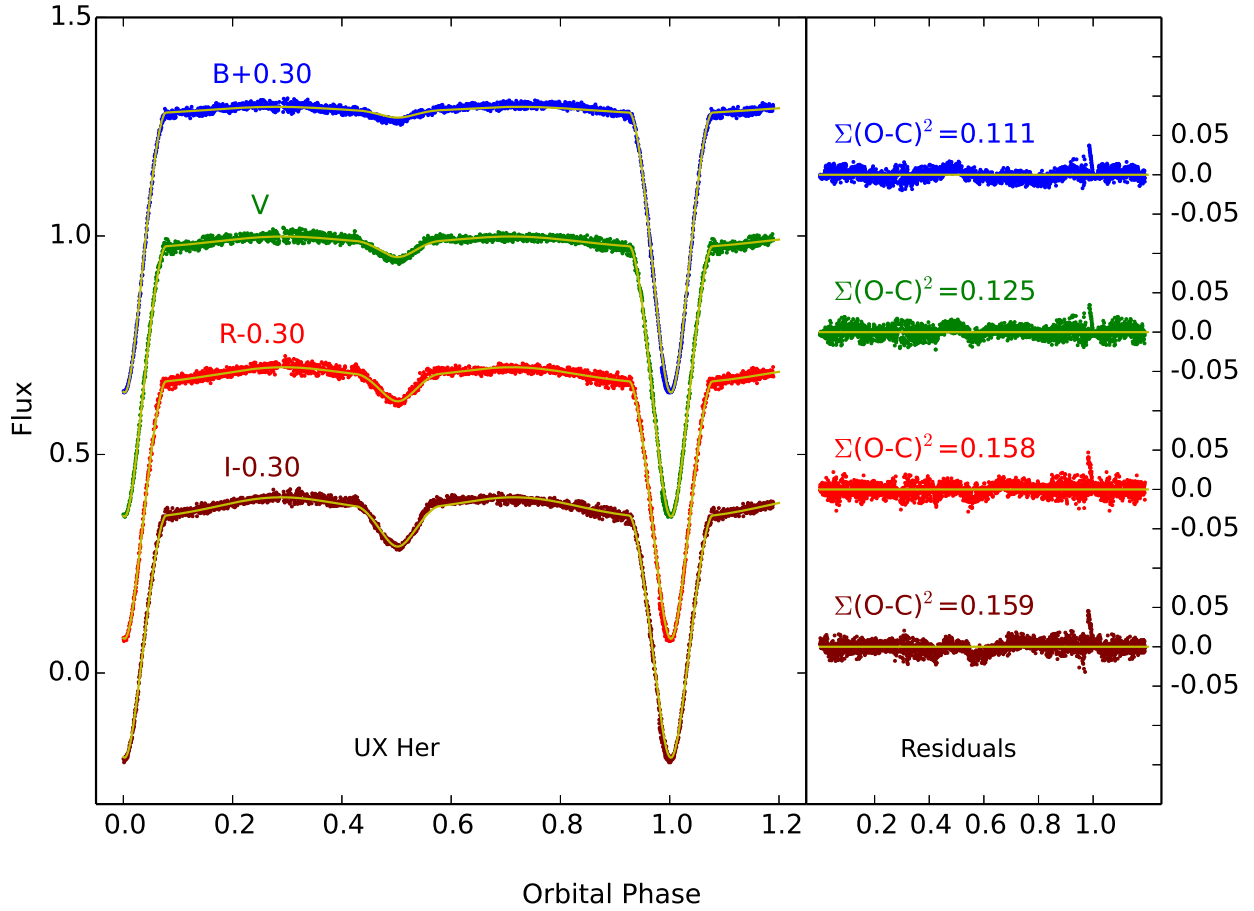


Fig. 4.— Same as in Fig. 3, but for UX Her

Table 3: Log of spectroscopic observations

System	Dates of Obs.	# of Data Pts.
XZ Aql	26,27 Sep 2009; 1,2 Oct 2010;	8
	8,9,10,11 Sep 2013	
UX Her	22,23,26 Apr 2011;	7
	7,11,12 Sep 2011	
AT Peg	26,27,28 Sep 2009; 5 Oct 2010;	9
	4 Sep 2011; 8 Sep 2013	

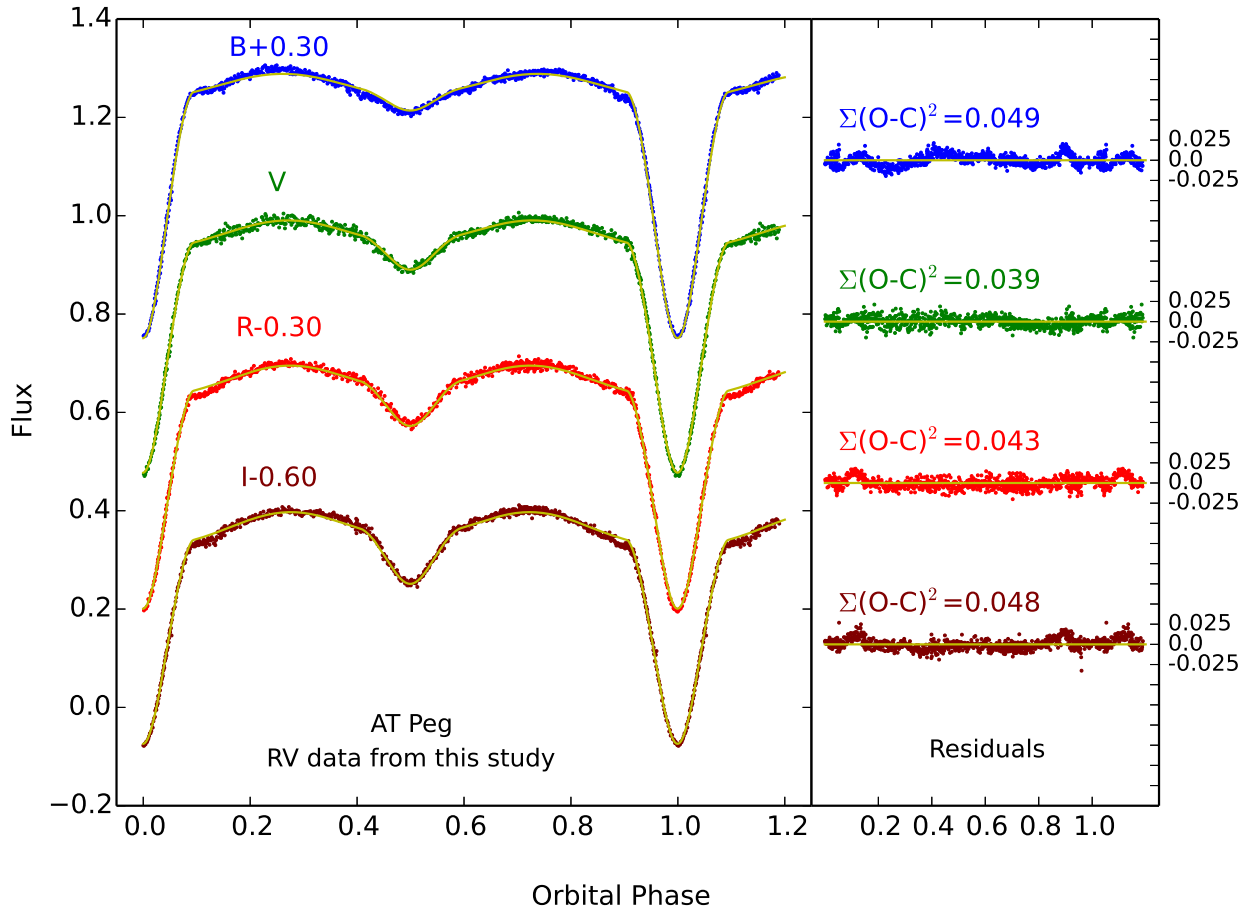


Fig. 5.— Same as in Fig. 3, but for AT Peg using our own measurements in DAO.

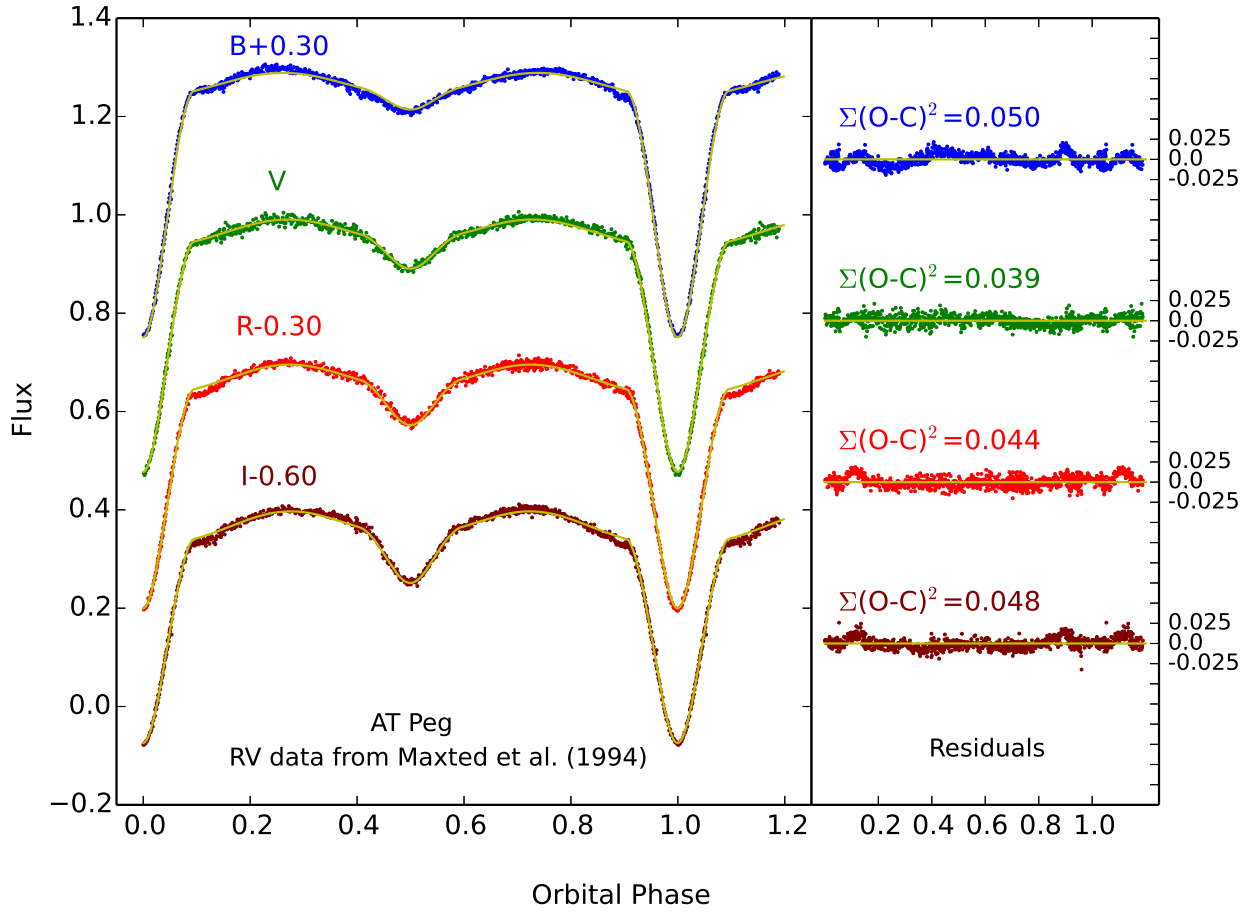


Fig. 6.— Same as in Fig. 3, but for AT Peg using Maxted et al. (1994)'s measurements.

Table 4: Results from the light curve analysis.*,**

Stellar Parameters	XZ Aql	UX Her	AT Peg	
			RV ₁	RV ₂
i [deg]	85.88(3)	82.28(2)	76.30(4)	76.25(4)
T_1 [K]	8770	8770	8360	8360
T_2 [K]	4744(5)	4478(5)	5057(6)	5051(6)
Ω_1	4.26(1)	4.55(1)	4.20(1)	4.22(1)
Ω_2	2.19(1)	2.19(1)	2.85(1)	2.85(1)
V_γ [km/s]	17.6(9)	-67.6(11)	10.0(19)	4.1(6)
$q = m_2/m_1$	0.184(4)	0.184(21)	0.484(3)	0.489(3)
Luminosities				
L_1 [B]	12.25(1)	12.25(1)	11.40(1)	11.40(1)
L_1 [V]	11.83(1)	11.87(1)	10.62(2)	10.61(2)
L_1 [R]	11.28(1)	11.32(1)	10.02(2)	10.01(2)
L_1 [I]	10.61(1)	10.70(1)	9.36(2)	9.34(2)
L_2 [B]	0.30	0.23	0.82	0.83
L_2 [V]	0.70	0.56	1.56	1.56
L_2 [R]	1.21	1.04	2.17	2.18
L_2 [I]	1.77	1.63	2.82	2.83

* Formal errors from the WD-code are in parantheses.

** Column RV₁ shows the results from the analysis using our own RV measurements, and RV₂ shows the same but using RVs from Maxted et al. (1994).

Table 5: Absolute Parameters.*

Parameter	XZ Aql	UX Her	AT Peg	
			RV ₁	RV ₂
$a[R_{\odot}]$	9.94(21)	8.00(9)	6.86(8)	6.91(7)
$\mathcal{M}_1[M_{\odot}]$	2.42(14)	2.42(12)	2.22(8)	2.26(7)
$\mathcal{M}_2[M_{\odot}]$	0.45(6)	0.44(6)	1.08(6)	1.11(5)
$\mathcal{R}_1[R_{\odot}]$	2.45(7)	1.84(5)	1.86(3)	1.87(3)
$\mathcal{R}_2[R_{\odot}]$	2.43(6)	1.96(5)	2.18(3)	2.20(3)
$M_{bol,1}$ [mag]	0.99(21)	1.61(11)	1.80(10)	1.78(9)
$M_{bol,2}$ [mag]	3.68(21)	4.40(11)	3.64(10)	3.62(9)
$\log g_1$ [cgs]	4.04(6)	4.29(5)	4.24(3)	4.25(3)
$\log g_2$ [cgs]	3.32(6)	3.50(5)	3.79(3)	3.80(3)

* Column RV₁ shows the results from the analysis using our own RV measurements, and RV₂ shows the same but using RVs from Maxted et al. (1994).

Table 6: Times of Minimum Light Levels Derived From Our Own Light Curves.

System	Time of Min. (HJD +2400000)	Error	Filter	Type
XZ Aql	56486.4291	0.0001	BVRI	primary
	56487.4975	0.0004	BVRI	secondary
UX Her	56089.4797	0.0003	BVRI	primary ¹
	56093.3568	0.0001	BVRI	secondary ¹
AT Peg	56146.5608	0.0001	BVRI	primary
	56153.4397	0.0016	BVRI	primary
	56157.4471	0.0005	BVRI	secondary
	55436.5775	0.0005	BR	secondary ²
	55439.4392	0.0004	BR	primary ²
	55442.2968	0.0008	BR	secondary ²
	55447.4616	0.0001	BR	primary ²

¹ Liakos & Niarchos (2010), ² Liakos et al. (2014)

variations were noticed that could be attributed to the light-time effect (LiTE) due to unseen additional components to these systems. For UX Her we found only cyclic variations that may be caused by a companion that is dynamically bound to the binary system. The parameters corresponding to companions of the three systems were derived using the equations based on the formulation of Irwin (1952, 1959). We checked the dynamical stability of the configurations by using the stability condition given by Harrington (1977) when an unseen third body was assumed to explain the periodic changes in the O-C diagrams. In each case the orbit of the third bodies has been assumed to be coplanar with that of the eclipsing pair. Errors have been estimated using a specific IDL code written by us. The results from the O-C analysis, including estimated mass transfer rate are given in Table 7. The errors were computed by propagating the observational errors on the results in the formal manner. We also give the initial light elements that we used in the computation of the orbital phases for each of the systems in this table before the results

4.3. Frequency Analysis

In order to search for potential pulsations in the data of the studied systems, we subtracted the theoretical light curves of the binary model from the corresponding observed ones and performed frequency analyses on the out-of-eclipse phases of the residuals with the software PERIOD04 v.1.2 (Lenz & Breger 2005) (for further details see Liakos et al. (2012b), Liakos & Niarchos (2013)). We searched for frequencies up to 80 cycles per day (c/d). After the first frequency computation the residuals were subsequently pre-whitened for the next one, until the detected frequency had a Signal-to-Noise Ratio (S/N) < 4 , which is the programme’s critical trustable limit. The l-degrees of the pulsation modes were identified with the software FAMIAS v.1.01 (Zima 2008) using theoretical δ Scuti models (MAD - Montalban & Dupret (2007)).

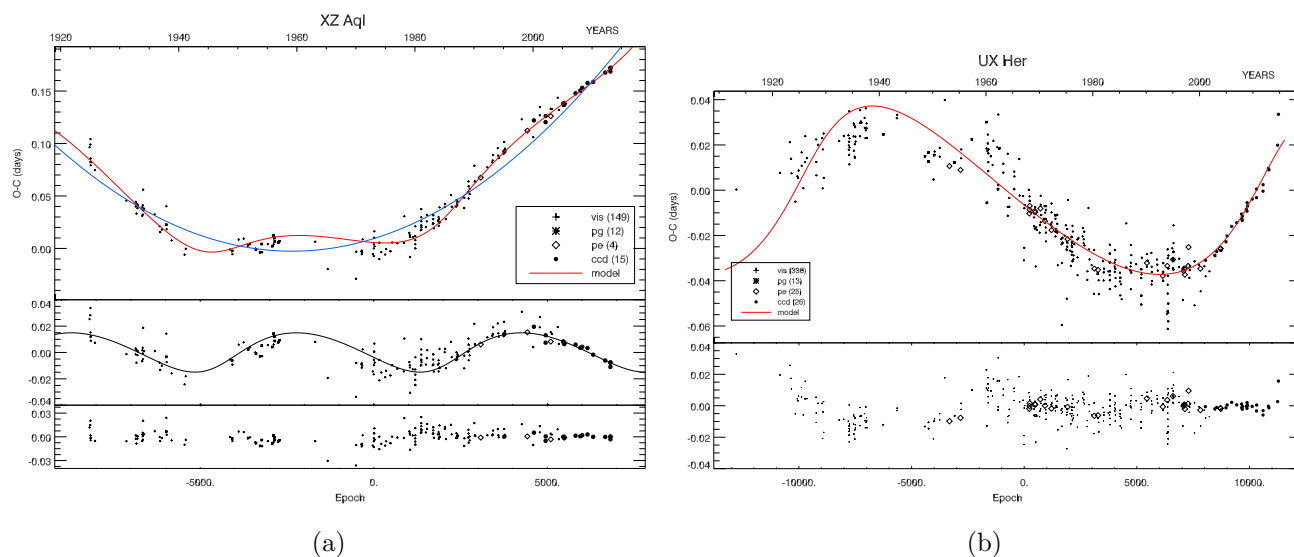


Fig. 7.— The O-C diagrams for XZ Aql (a) and UX Her (b). The fits are plotted as solid lines (best fit models in blue and parabola fits superimposed by sinusoidal variations in red in the electronic version). Residuals from the fits are given in the lower panels. Symbols have been defined in the legends.

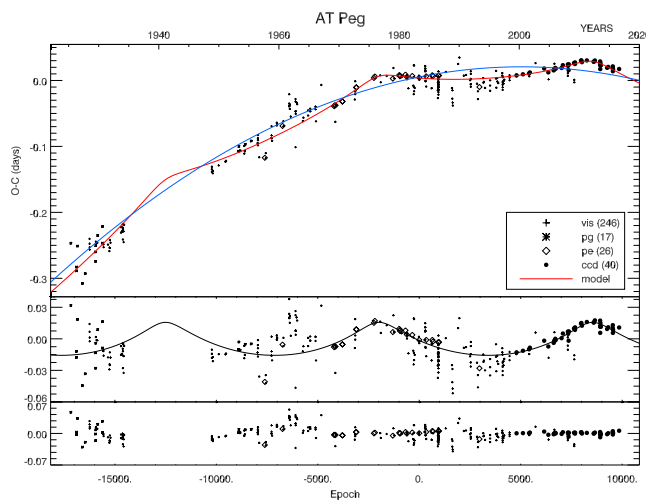


Fig. 8.— Same as the Fig. 7, but for AT Peg

Table 7: Results from the O-C analysis.

	XZ Aql	UX Her	AT Peg
T_o (HJD)	2441903.4610 ¹	2439672.3760 ²	2445219.8512 ¹
P (days)	2.139181	1.548853	1.1460764
dM/dt [M_\odot /year]	6.37(13) $\times 10^{-8}$	-	-
dP/dE [days/cycle]	4.33(5) $\times 10^{-9}$	-	-1.21(1) $\times 10^{-9}$
P_3 [years]	37.97(96)	86.81(52)	33.02(41)
A [days]	0.015(1)	0.037(2)	0.016(1)
ω [$^\circ$]	316(18)	18(1)	86(11)
e	0.21(10)	0.41(7)	0.53(8)
$a_{12}\sin(i)$ [AU]	2.62(150)	6.99(16)	2.72(90)
$f(m_3)$ [M_\odot]	0.01(2)	0.045(3)	0.02(2)
$M_{3,min}$ [M_\odot]	0.52(8)	0.87(7)	0.68(5)

¹ Samus et al. (2012), ² Tremko et al. (2004)

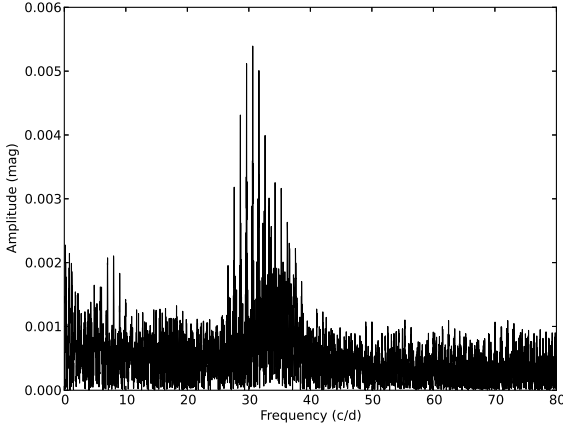
UX Her and AT Peg did not show any evidence of pulsating behaviour. For XZ Aql we found two frequencies in the range 30-36 c/d. By taking into account the temperature of the primary component (8770 K), the frequency range (3-80 c/d - Breger (2000)), and the spectral types of the δ Sct stars (A-F), it can be plausibly suggested that this component is a δ Sct type pulsator. The pulsation signal is present in all filters, and its amplitude decreases from B to I . Frequency analysis includes ~ 1300 points per filter coming from 19 nights of observations in a time span of 73 days. The data of the first 17 nights were obtained in a time span of 28 days, sufficient to detect quick-pulsation modes. Finally, given that the system is a conventional semi-detached system (i.e. the more massive component, the pulsator in this case, is the mass gainer), it can be also categorized as a typical oEA system (Mkrtychian et al. 2002). Furthermore, two more frequencies were found (0.50 and 0.93 c/d) but they were also detected with approximately the same values in the comparison-check light curves. So, we conclude that their origin is not connected with the true pulsations, and they can be considered as artifacts (e.g. observational drift). Table 8 includes the frequency values (f), the amplitudes (A), the phases (Φ), the S/N, and the l -degrees. In Fig. 9 the periodogram, and the Fourier fit on the data of an individual night are presented. Although the observed amplitude is rather low to reach a firm conclusion, there are more than one frequency with sufficient S/N in the range where δ Scuti stars pulsate and the beating seems to be obvious. More precise future observations will provide further evidence for the existence of heat-driven pulsations in this system.

4.4. Evolutionary Status

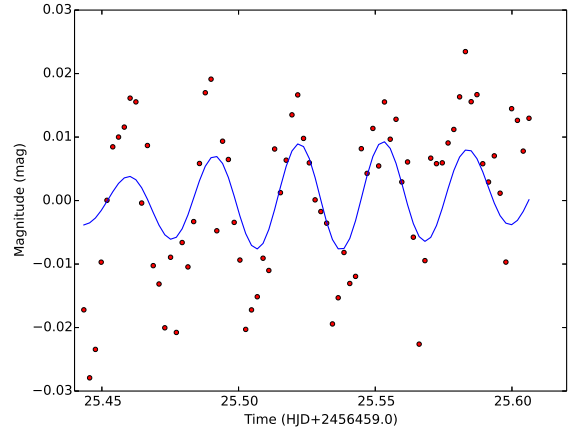
We used the Geneva stellar models (Ekström et al. 2012) to investigate the evolutionary states of the components of all the studied systems. We generated a grid of evolutionary

Table 8: Results from the frequency analysis on XZ Aql data.

l-degree	Filter	f [c/d]	A [mmag]	Φ [2π rad]	S/N
3	<i>B</i>	30.631(1)	5.4(4)	0.51(1)	7.8
	<i>V</i>	30.633(1)	4.4(4)	0.46(1)	8.1
	<i>R</i>	30.632(1)	3.2(4)	0.48(2)	5.3
	<i>I</i>	30.635(1)	2.6(3)	0.44(2)	7.9
0	<i>B</i>	35.247(1)	3.2(4)	0.64(2)	4.0
	<i>V</i>	35.250(1)	2.4(3)	0.57(2)	4.2
	<i>R</i>	35.289(1)	1.9(4)	0.73(3)	4.3
	<i>I</i>	35.240(1)	1.9(3)	0.81(2)	3.9



(a)



(b)

Fig. 9.— (a) The periodogram of the *B* filter data of XZ Aql, where the two detected frequencies in the range 30–36 c/d are shown. (b) Fourier fit on the longest data set for XZ Aql recorded on the day (JD 2456459) with the *B* filter.

tracks for a suitable range of fixed masses spanning the measured values, by making use of interactive tools provided by a web interface¹. We fixed metallicity at solar composition ($Z = 0.014$) and generated non-rotating models. In order to populate the Hertzsprung-Russell diagram (HRD) with observed stars in detached, semi-detached and near-contact eclipsing binaries, we collected the parameters of components in detached systems from Torres et al. (2010) and those in semi-detached binaries from Surkova & Svechnikov (2004). From both catalogues we have selected only the binaries with spectroscopically determined mass ratios. In Fig. 10 we show the computed Geneva evolutionary tracks, parameters of components of selected detached binaries (primaries are indicated with filled while secondaries with unfilled triangles), semi-detached and near-contact binaries (primaries are indicated with filled, secondaries with unfilled circles) and our program stars (indicated with marks selected according to their nature and component type and in red color in the electronic version) on the HRD. We also present the Mass-Luminosity (MLD) and Mass-Radius (MRD) diagrams in Fig. 11 following the same symbol types as these used in Fig. 10. It should be borne in mind that the stellar models are valid only for single stars, or stars in binaries which do not interact strongly, while the stars in our sample can not be assumed to be free from stellar interactions in a binary system. The implications of this fact are clear when the positions of the evolved secondary components in these systems are compared with the evolutionary tracks given for their masses because they transfer material to their more massive and rather unevolved counterparts. The lines indicating the positions of the Zero Age Main Sequence (ZAMS) and the Terminal Age Main Sequence (TAMS) are shown in these figures. ZAMS is defined as the time when the hydrogen mass fraction in the center (X_c) has decreased by 0.25% for a newborn star with the solar composition while TAMS is set at the time when X_c will be of the value 10^{-5} for a star starting its life with solar composition. Following the

¹<http://obswww.unige.ch/Recherche/evoldb/index/>

above definition, a star will be on the ZAMS when thermal equilibrium is achieved and the star has burnt 0.25% of its hydrogen in the core (Ekström et al. 2012; Mowlavi et al. 2012).

5. Results & Discussion

In this study we have performed thorough analyses of the light curves and period variations of three close binary systems. Analysis of our light curves was based on combined photometric and spectroscopic data. The mass ratios of the studied systems were determined from our own spectroscopic observations. We made use of the Wilson-Devinney algorithm to derive the best fits to new, multicolor light curves, and based on obtained results we calculated the absolute parameters of components. The complementary information about the systems has been derived by analyzing their period behaviour.

5.1. XZ Aql

The light curve of XZ Aql has equal levels of light maxima, and we were able to obtain its solution that required neither a spot nor a third light. This is a high inclination ($i=86$ deg), semi-detached binary with the less massive secondary filling its Roche lobe, while the primary component is well inside its Roche lobe. The frequency analysis performed after having removed the binarity effects from its light curves hints that this A-type primary is a δ Sct type pulsator. Due to a significant temperature difference between components, the contribution of the secondary star to the total system light is small: only 2% in the B filter and about 13% in the I filter.

From the O-C analysis we found a parabolic change in the eclipse timings combined with a periodic variation that could be due to an unseen third body as previously suggested

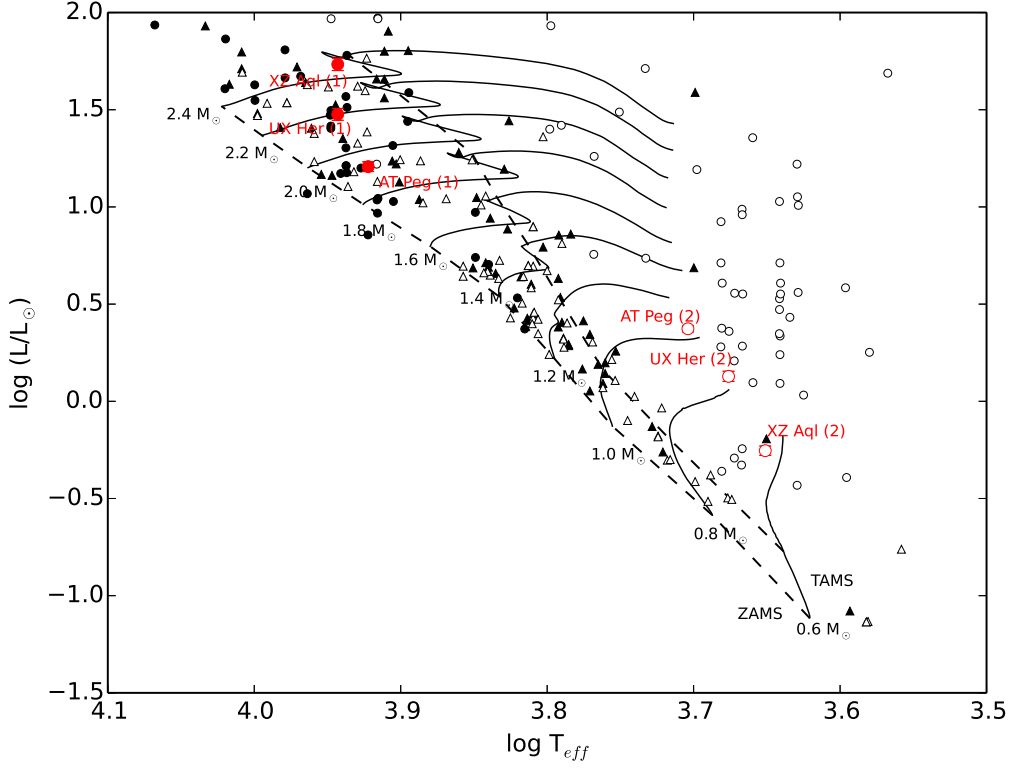


Fig. 10.— The positions of detached (primaries in filled, secondaries in unfilled triangles) and semi-detached (primaries in filled, secondaries in unfilled circles) binaries in the HRD. Parameters of detached systems taken from Torres et al. (2010), while these for semi-detached ones from Surkova & Svechnikov (2004). Parameters of stars analyzed in this work are marked with larger symbols (red colored in the electronic version). The evolutionary tracks for a dense grid of masses, done by interpolation between the existing tracks of the Geneva stellar models for the mass range 0.5-3.5 M_{\odot} (Mowlavi et al. 2012), are plotted with lines. ZAMS and TAMS are also indicated with dashed lines. The location of the components of AT Peg is based on the absolute measurements from the WD fits using our own radial velocity observations.

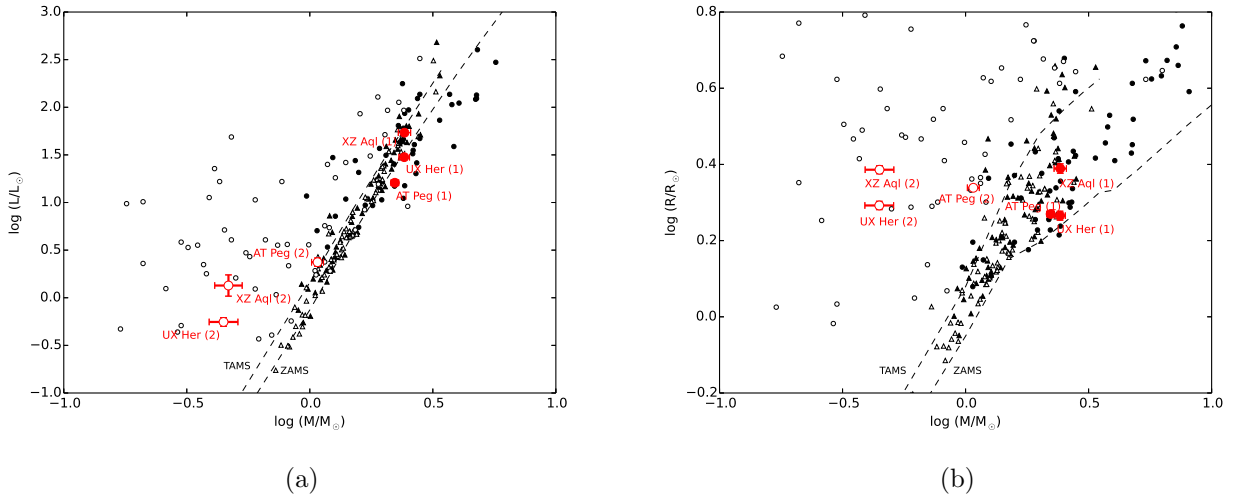


Fig. 11.— Mass-Luminosity (a) and Mass-Radius (b) diagrams. ZAMS and TAMS computed from the theoretical models by Ekström et al. (2012) are plotted by dashed lines. Positions of components in detached, semi-detached and these in systems derived in this work are also shown. Symbols meaning is the same as in Fig. 10.

by Soydugan et al. (2006). We made trial computations with a third light, however, its resulting intensity was negligible, reaching only 1% in the I filter. Assuming that this third body is in coplanar orbit with the binary and that it is an MS star, its luminosity contribution to the total light would only be 0.2%. We found that the orbit of this third companion would be stable according to Harrington’s criterion (Harrington 1977). We have found a parabolic relation in the residuals that may be due to mass transfer from the less massive component to the more massive one. When the corresponding orbital period changes are removed, one might argue that there is a possibility of a second periodicity in the O-C points, but the number of data points is not sufficient to prove it. Alternatively, the periodic variation of the orbital period could also be explained with the quadrupole moment variation of the secondary.

Our results from the orbital period variation analysis also support the finding that the secondary component fills its Roche lobe and transfers mass to the more massive primary conservatively. The positions of its component on the HRD, MLD, and MRD based on the absolute parameters computed for each of the components as a result of the light curve modeling support this finding. Both the computed masses and the effective temperatures from our fit are qualitatively consistent with evolutionary tracks, which also point to a main-sequence primary half way between the ZAMS and the TAMS with $\sim 2.42 M_{\odot}$, and an evolved red giant secondary, somewhat more massive ($\sim 0.65 M_{\odot}$) than our computed value ($\sim 0.45 M_{\odot}$). This discrepancy can be explained by the mass transfer from the secondary to the primary star, the time scale of which should be less than 10 Myr assuming a constant rate for the mass transfer. The fact that the main sequence primary has not gained all the mass the secondary transfers can only be explained by a non-conservative mass loss.

5.2. UX Her

Our light curve modelling for UX Her used the new value for the spectroscopic mass ratio resulting from our DAO data $q_{sp} = 0.184$. It is significantly smaller than the previous determination from photometry alone as a result of the q -search by (Djurašević et al. 2006). We obtained a semi-detached configuration for this system with the less massive component filling its Roche lobe while the primary being well within it. Therefore, mainly due to the lower q value, the derived secondary mass is also smaller than that previously found (Lazaro et al. 1997; Djurašević et al. 2006), both considered this system as a detached one based on either photometrically or spectroscopically determined mass ratios from photographic plates. The evolutionary state of UX Her components deduced from their positions on the HRD, MLD and MRD diagrams point to the interpretation that the primary star is still on the main sequence, while the secondary is the more evolved star.

We did not find a significant quadratic component to the period variation, therefore we conclude there is no evidence of mass transfer. The cyclic period variations can more plausibly be explained by a third body of mass $M_3 = 0.87 M_\odot$, orbiting the center of mass on a significantly eccentric orbit ($e = 0.41$). Tremko et al. (2004) found a smaller mass, less than half of the value that we found ($0.30 M_\odot$). As a test, we also performed computations adding a third light as a free parameter. It turned out that contribution of this hypothetical tertiary to the total light is negligible: it reached about 1% only in the I filter so therefore we present the solution without l_3 as the final one. If we assume that this body has a coplanar orbit with that of the eclipsing binary and that it is an M5 star, its luminosity contribution will be less than 1% (0.75% according to our calculations), which is below our detection limits with the photometry. Previously Selam & Albayrak (2007) also found cyclic changes in the orbital period in UX Her. They attributed the variation to magnetic

activity, which would also explain the observed asymmetries in the light curve. However, the latest CCD data have a very low scatter around our best fit. More scatter would be expected in the case of magnetic activity because it would complicate the measurement of the eclipse times from asymmetric minimum profiles due to the surface spots therefore causing more errors. Further observations of the system covering a longer time base will be needed to make sure that the period and the amplitude of the variation change from one cycle to another, which would be the case in the presence of strong magnetic activity. Otherwise, the variation could be argued to cause from the gravitational pull of an unseen third body. In addition, the temperature of the primary is too high (8770 K) to expect cool surface spots. Though it would be somewhat reasonable to locate spots on the cooler secondary, our non-spotted solution satisfactorily fits the observations. Therefore, we give here only the third body solution because we do not have further evidence (e.g. variations in magnetic activity indicators) supporting the magnetic activity argument. Moreover, the dynamical stability test according to Harrington’s criterion (Harrington 1977) points to a stable orbit for the suggested third body, thus supporting the second hypothesis.

5.3. AT Peg

Light curve modelling for AT Peg proceeded without difficulty for both radial velocity data sets (our own and that of Maxted et al. (1994)). A convergence was quickly found for a model that required neither a third light nor a spot. Theoretical light curves fit observed ones very well with just very small discrepancies visible around the primary minimum but only in *B* and *I* filters. We arrived at the semi-detached solution with the less massive secondary filling the Roche lobe and the primary well within it. Absolute parameters and their errors differ only within a few percent between the two models obtained by using two different radial velocity data sets.

The O-C analysis shows a parabolic trend. A periodic relation for the residuals can also be asserted. The quadratic term cannot be interpreted as being due to conservative mass transfer between components as it would require the more massive star to be the mass loser, in contradiction with the results from light curve modeling. This discrepancy can be explained by non-conservative mass loss from the system or losing of angular momentum via magnetic breaking. Such systems with orbital period decrease may be the progenitors of contact binaries (Bradstreet & Guinan 1994; Qian 2000), because the fill-out factor of the primary may increase while the orbital period decreases, eventually causing the primary to fill its Roche lobe. We do not have evidence for strong magnetic activity such as light curve modulations and asymmetries in the light curves due to stellar spots. The spectral window of our spectral observations is also limited to 5000-5250 Å region, where we have not observed a signature of activity or stellar wind in the resolution our spectra were taken. The spectral type of the primary (A4) would not support this argument either, assuming it is a normal star without any kind of peculiarity. The positions of the components relative to the evolutionary tracks on the HRD indicate that the primary might have lost some mass. The evolutionary model value with no mass transfer is $\sim 1.90 M_{\odot}$ for the primary component, while the computed mass from the light curve analysis is $2.22 M_{\odot}$ and the mass of the secondary is consistent in both models ($\sim 1.08 M_{\odot}$).

The residuals from the quadratic fit may be alleged to follow a periodic behavior, which can be attributed to an unseen body ($M_{3,min} = 0.68 M_{\odot}$) gravitationally bound to the system, orbiting its center of mass once in every ~ 33 years on a significantly eccentric ($e = 0.53$) orbit. The relatively low mass of the tertiary can explain its negligible contribution to the total light. Additional bodies have been plausibly argued to extract momentum from the

binary, causing the orbit to shrink and hence the orbital period to decrease (Yang & Wei 2009). This could be at least a part of the reason that causes a period decrease although the direction of the mass transfer is towards the more massive primary.

6. Acknowledgments

This work was partially supported by the NCN grant No. 2012/07/B/ST9/04432. This work was performed in the framework of PROTEAS project within GSRTs KRIPIS action for A.L., funded by Greece and the European Regional Development Fund of the European Union under the O.P. Competitiveness and Entrepreneurship, NSRF 2007-2013 and the Regional Operational Program of Attica. We gratefully acknowledge invaluable discussions with Prof. Selim O. Selam and his suggestions. We thank Prof. Slavek Rucinski for his comments on the broadening function. We also thank all the observers participating in the observations of our targets, and the staff members at the DAO and UoA.

REFERENCES

- Ashbrook J., 1952, AJ, 57, 259
- Berry R., Burnell J., 2000. The Handbook of AIP. Richmond (Virginia)
- Borkovits T., Hegedus T., 1995, POBeo, 49, 97
- Borkovits T., Hegedus T., 1996, A&AS, 120, 63
- Bradstreet D. H., Guinan E. F., 1994, ASPC, 56, 228
- Breger M., ASPCS, 210, 3
- Cannon A.J., 1922, HarCi, 231, 1
- Cannon A. J., Pickering E. C., 1924, AnHar, 99, 1
- Cester B., Fedel B., Giuricin G., Mardirossian F. Mezzetti M., Predolin F., 1979, MmSAI, 50, 553
- Claret A., Bloemen S., 2011, A&A, 529, 75
- Claret A., Hauschildt P. H., Witte S., 2012, A&A, 546, 14
- Claret A., Hauschildt P. H., Witte S., 2013, A&A, 552, 16
- Cristaldi S., Walter K., 1963, AN, 287, 103
- Cristaldi S., Walter K., 1965, MmSAI, 36, 197
- Djurašević G., Rovithis-Livaniou H., Rovithis P., Georgiades N., Erkapić S., Pavlović R., 2006, A&A, 445, 291
- Erleksova G. E., 1959, PZ, 12, 293

- Ekström S., Georgy C., Eggenberger P., Meynet G., Mowlavi N., Wyttenbach A. , Granada A., Decressin T., Hirschi R., Frischknecht U., Charbonnel C., Maeder A., 2012, A&A, 537, A146
- Giuricin G., Mardirossian F.,1981, ApJS, 46, 1
- Giuricin G., Mardirossian F., Predolin F., 1981, A&AS, 43, 251
- Gordon K. C., Kron, G. E., 1963, PASP, 75, 412
- Gordon K. C., Kron, G. E., 1965, AJ, 70, 100
- Gudur N., Sezer C., Gülmen O., 1987, IBVS, 297, 1
- Gülmen O., Gudur N., Sezer C., 1993, Ap&SS, 206, 259
- Guthnick P., Prager R., 1931, AN, 244, 81
- Hanna M. A, 2012, NRIAG Journal of Astronomy and Geophysics, 1, 87
- Harmanec P., 1988, BAICz, 39, 329
- Harrington R.S.,1977, RMxAA, 3, 139
- Hilditch R. W., Hill G., 1975, MmRAS, 79, 101
- Hill G., Barnes J. V., 1972, PASP, 84,430
- Hill G., Hilditch R. W., Younger F., Fisher W. A., 1975, MmRAS, 79, 131
- Hroch F., 1998, Proceedings of the 29th Conference on Variable Star Research, 30
- Irwin J.B., 1952, ApJ, 116, 211
- Irwin J.B., 1959, ApJ, 164, 149

Kaho S., 1952, TokAB, II, 49

Koch J. C., Koch R. H, 1962, AJ, 67, 462

Kurzemnietsē I. A., 1952, Tr. Akad. Nauk Latvian SSR 3, 73

Kwee K. K., van Woerden, H., 1956, BAN, 12, 327

Lassovszky K., 1935, AN, 256, 167

Lazaro C., Martinez-Pais I. G., Arevalo M. J., Antonopoulou E., 1997, AJ, 113, 1122

Lenz P., Breger, M., 2005, CoAst, 146, 53

Liakos A., Niarchos P., 2010, IBVS, 5958

Liakos A., Niarchos P., Budding E., 2012a, IAUS, 282, 55

Liakos A., Niarchos P., Soydugan E., Zasche P., 2012b, MNRAS, 422, 1250

Liakos A., Niarchos P., 2013, Ap&SS, 341, 123

Liakos A., Gazeas K., Nanouris N., 2014, IBVS, 6095

Mardirossian F., Mezzetti M., Predolin F. and Giuricin G., 1980, A&AS, 40, 57

Margrave T. E., 1981, IBVS, 1930, 1

Maxted P. F. L., Hill G., Hilditch R. W., 1994, A&A, 285, 535

Mkrtichian D.E., Kusakin A.V., Gamarova A.Yu., Nazarenko V., 2002, ASPCS, 259, 96

Montalban J., Dupret M.-A., 2007, A&A, 470, 991

Motl D., 2004, C-MUNIPACK, <http://c-munipack.sourceforge.net/>

- Mowlavi N., Eggenberger P., Meynet, G., Ekström S., Georgy C., Maeder A., Charbonnel C., Eyer L., 2012, *A&A*, 541, 41
- Nelson R.H., 2010a, Software by Bob Nelson.
(<http://members.shaw.ca/bob.nelson/software1.htm>)
- Nelson R.H., 2010b, Spectroscopy for Eclipsing Binary Analysis in The Alt-Az Initiative, Telescope Mirror & Instrument Developments, Collins Foundation Press, Santa Margarita, CA, Genet, R.M., Johnson, J.M., and Wallen, V. (eds)
- Nelson R.H., Şenavcı, H.V., Baştürk, Ö, Bahar, E., 2014, *NA*, 29, 57
- Obůrka O., 1964a, *BAICz*, 15, 26
- Obůrka O., 1964b, *BAICz*, 15, 250
- Obůrka O., 1965, *BAICz*, 16, 212
- Pickering E. C., 1908, *AN*, 179, 7
- Pokorný Z., Zlatuška J., 1976, *BAICz*, 27, 341
- Qian S. 2000, *AJ*, 119, 901
- Rucinski S. M., 2004, Proceedings of the IAU Symposium 215
- Rügemer H., 1934, *AN*, 251, 307
- Samolyk G., 1996, *JAVSO*, 24, 99
- Samus N.N., Durlevich O.V., Kazarovets E V., Kireeva N.N., Pastukhova E.N., Zharova A.V., et al., General Catalogue of Variable Stars (Samus+ 2007-2012)
- Sanford R. F., 1937, *ApJ*, 86, 153

Sarna M. J., Muslimov A., Yerli S. K., 1997, MNRAS, 286, 209

Savedoff M. P., 1951, AJ, 56, 1

Schneller H., 1931, AN, 242, 177

Selam S. O., Albayrak B., 2007, AN, 328, 154

Surkova L. P., Svechnikov M. A., 2004, Vizier Online Data Catalog: V/115

Soydugan F., Soydugan E., İbanoğlu, 2006, AN, 327, 705

Torres G., Andersen J., Giménez A., 2010, A&ARv, 18, 67

Tremko J., Kreiner J. M., Pribulla T., 2004, CoSka, 34, 337

Tsesevich V. P., 1944, Astron. Circ. USSR, 27, 6

Tsesevich V. P., 1954, OAP, 4,

van Genderen A. M., 1962, BAN, 16, 151

Van Hamme W., Wilson R.E., 2007, ApJ, 661, 1129

Wilson R. E., Devinney E. J., 1971, ApJ, 166, 605

Wilson R. E., 1979, ApJ, 234, 1054

Wilson R. E., 1990, ApJ, 356, 613

Wilson R. E., 2008, ApJ, 672, 575

Wilson R. E., 2012, ApJ, 144, 73

Wilson R. E., Van Hamme, W., Terrell, D., 2010, ApJ, 723, 1469

Witkowski J., 1925, AcA, 9, 1

Wood B. D., Forbes J. E., 1963, AJ, 68, 257

Yang Y.-G., Wei J.-Y., 2009, ApJ, 137,226

Zima W.,2008, CoAst, 155,1

Zinner E., 1913, AN, 195, 453

Zola S., Şenavcı H. V., Liakos A., Nelson R. H., Zakrzewski B., 2014, MNRAS, 437, 3718